Scaling of the rupture dynamics of polymer chains pulled at one end at a constant rate

S. Fugmann and I. M. Sokolov
Institut für Physik, Humboldt-Universität Berlin, Newtonstrasse 15, 12489 Berlin, Germany
(Received 17 July 2008; revised manuscript received 4 November 2008; published 13 February 2009)

We consider the rupture dynamics of a homopolymer chain pulled at one end at a constant loading rate r. Compared to single bond breaking, the existence of the chain introduces two aspects into rupture dynamics: The non-Markovian aspect in the barrier crossing and the slow down of the force propagation to the breakable bond. The relative impact of both these processes is investigated, and the second one was found to be the most important at moderate loading rates. The most probable rupture force is found to decrease with the number of bonds as $f_{\max} \propto -[\ln(\text{const}\, N/r)]^{2/3}$ and finally to approach a saturation value independent on N. All of our analytical findings are confirmed by extensive numerical simulations.

DOI: 10.1103/PhysRevE.79.021803 PACS number(s): 82.37.−j, 05.40.−a

I. INTRODUCTION

Modern developments of micromanipulation techniques made possible the experiments on the mechanical response of single molecules to a well-defined load. The typical setup here corresponds to the force growing linearly in time until the molecule breaks or changes its structure. Examples are the molecular failure experiments [1–6] and the ones on protein unfolding [7]. The dynamic force spectroscopy [7,8] delivering the spectrum of the rupture force versus the loading rate offers a powerful tool to determine the bonds' strengths and gives deep insights into the internal dynamics of molecules [9–12]. In all of these experiments polymers play an outstanding role, either as elastic couplers or as a subject of study [5,13,14]. Reference [14] reports a strong impact of the polymer size on its rupture dynamics. Furthermore, it was shown, that even the mechanical properties of passive polymer spacers can affect the outcome of pulling experiments [5,6,13].

The theoretical description concentrates on breaking of one (presumably the weakest) bond and fully disregards the chain structure of the system. From the theoretical point of view the rupture of a single bond under a constant loading rate can be described as a thermally activated escape from a time-dependent potential well [10,11,15–17]. Approximating the energy landscape close to the barrier up to the third order Ref. [10] predicts that the rupture force scales like $-[\ln(\text{const}\, R)]^{2/3}$, with R being the loading rate. Numerical simulations show that this prediction performs better than the one of a linear theory [8,15], particularly in the strong pulling limit [16,17]. On the other hand, the situation of breaking of the more or less homogeneous chain has hardly been considered theoretically. Thus, Ref. [12], in addition to consider an attached chain of different bonds, discusses breaking of a ring of identical bonds, i.e., of a chain with periodic boundary conditions. Although the experimental realization of this situation is possible in the setup discussed in Ref. [18], it does not correspond to the typical situation. In what follows we therefore concentrate on a chain pulled at one end with another end clamped.

For sufficiently low loading rates each bond experiences the same force and the rupture can occur at an arbitrary bond—the situation of Refs. [12,18] is recovered. For a high loading rate the actual force profile along the chain is inhomogeneous since the time of the order of the Rouse time τ_R [19] is necessary for the stress to propagate through the chain. If bond rupture occurs on a time scale shorter than the Rouse time, only a part of the chain is under stress and accounts for the rupture process. Thus the rupture force will be crucially affected by the number of monomers in the chain.

This paper is organized as follows: In the next section we introduce the chain model and recall in Sec. III the rupture dynamics of a single Morse bond under constant loading. In Sec. IV we study the rupture dynamics of the chain. Finally we summarize our results.

II. MODEL

Our model corresponds to a chain of monomers interacting via the Morse potential $U(q)$ given by

$$U(q) = \frac{C}{2\alpha}(1 - e^{-\alpha q})^2, \tag{1}$$

with dissociation energy $C/(2\alpha)$ and stiffness $C\alpha$ as a prototype of intramolecular interaction potential offering fragmentation. Otherwise, the model is identical to the Rouse one [19]: We disregard hydrodynamical interactions and describe the interaction of the monomers with the heat bath via independent white noises. The constant loading enters through an additional time-dependent potential of the form

$$L(q,t) = -qRt, \tag{2}$$

with loading rate R. The load is denoted by $F(t) = -\partial L(q,t)/\partial q$ and is applied to one end of the chain while the other end is fixed.

III. SINGLE BOND RUPTURE DYNAMICS

Let us first recall the rupture dynamics of a single Morse bond under constant loading [10,11,20–22]. At smaller loads the overall potential has two extrema, a minimum corresponding to a metastable state of the pulled bond, and a maximum providing the activation barrier. There exists a critical load $F_i = F(t_i) = C/4$ for which the extrema merge at

$q_i = \ln(2)/\alpha$ and disappear. In the purely deterministic dynamics the Morse bond breaks exactly at $t_i = F_i/R$. Since the system is in contact to a heat bath at temperature T, its overdamped dynamics is described by

$$\dot{q} = \frac{C}{\gamma}(1 - e^{-\alpha q})e^{-\alpha q} + \frac{R}{\gamma}t + \sqrt{\frac{2k_BT}{\gamma}}\xi(t), \tag{3}$$

with $\xi(t)$ being Gaussian white noise and friction coefficient γ. We introduce $c = C/\gamma$ ($[c] = \mathrm{nm}/\mu\mathrm{s}$), $r = R/\gamma$ ($[r] = \mathrm{nm}/\mu\mathrm{s}^2$), and $f = F/\gamma$ (in the following f is referred to as force). The diffusion coefficient is denoted by $D = k_BT/\gamma$ ($[D] = \mathrm{nm}^2/\mu\mathrm{s}$).

The probability $W_1(t)$ that the bond remains intact can be expressed through the following kinetic equation [10,11,20,22] $dW_1(t)/dt = -k(t)W_1(t)$, with $k(t)$ being the Kramers rate [23,24]. Taking $f = rt$ we can rewrite the kinetic equation in the form

$$\frac{dW_1(f)}{df} = -\frac{1}{r}k(f)W_1(f). \tag{4}$$

The measured probability density functional (PDF) for the rupture forces $P_1(f)$ then is

$$P_1(f) = -\frac{dW_1(f)}{df}. \tag{5}$$

Under the assumption that f is close to f_i when bond rupture occurs, it is usual to expand the potential around the inflection point q_i up to the third order in deviations from q_i [9–11]. We note that the breakdown properties of the chain only depend on the behavior of the potential close to the point of critical load, which are universal [11,16,17]. Using the Morse potential simply gives a convenient parametrization of the situation in terms of dissociation energy and stiffness. The Kramers rate becomes

$$k(f) = \frac{c\alpha}{4\pi}\sqrt{1 - \frac{f}{f_i}}e^{-(c/3\alpha D)[1 - (f/f_i)]^{3/2}}. \tag{6}$$

Solving (4) one derives

$$W_1(f) = W_0 \exp\left\{-\frac{v}{r}\exp\left[-w\left(1 - \frac{f}{f_i}\right)^{3/2}\right]\right\} \tag{7}$$

with $v = c\alpha^2 D/(8\pi)$ and $w = c/(3\alpha D)$. The normalizing prefactor is

$$W_0 = \exp\left(\frac{v}{r}e^{-w}\right). \tag{8}$$

In the limit of small loading rates the most probable rupture force $f_{\max}$ follows the scaling relation [9,10]:

$$f_{\max} = f_i\left[1 - \left(\frac{\ln\left(\frac{v}{r}\right)}{w}\right)^{2/3}\right]. \tag{9}$$

IV. CHAIN OF N BONDS

Let us now turn to a chain of N bonds. To be concrete and to illustrate the viability of the effects we chose some typical experimental parameter values [15,25,26] $-C/(2\alpha) = 3.5 \times 10^{-19}$ J with $\alpha = 10^{10}$ m^{-1}, $k_BT = 4 \times 10^{-21}$ J, the friction coefficient $\gamma = 2 \times 10^{-6}$ kg/s, and a loading rate $R = 10^{-7}$ N/s. This experimentally relevant loading rate corresponds to $r \sim 10^{-4}$ nm/μs^2 in our calculations. The estimates show that the effects discussed below are important for chains consisting of less then 10^3 monomers.

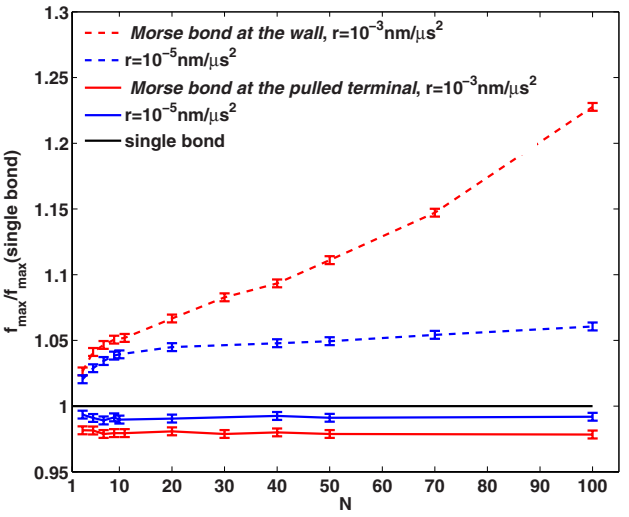

FIG. 1. (Color online) Most probable rupture force $f_{\max}$ for a single breakable Morse bond situated at the fixed (dashed lines) or at the pulled end (solid lines) of a chain of $N-1$ harmonic springs as a function of N. Red lines correspond to $r = 10^{-3}$ nm/μs^2 while the blue lines correspond to $r = 10^{-5}$ nm/μs^2. The flat solid line shows the value of $f_{\max}$ for a single bond, given by Eq. (9). The parameter values are $c = 3.5$ nm/μs, $D = 2 \times 10^{-3}$ nm^2/μs, and $\alpha = 10$ nm^{-1}. Error bars indicate the uncertainty due to the binning of numerical data.

A. Chain with a single breakable bond

To get insight into the role of the chain we consider first the situation when only one bond is breakable and take this bond to be either at the fixed or at the pulled end of the chain. The rest of the chain is considered as a harmonic Rouse one. The influence of the chain on the breaking properties of the bond is twofold: First, due to the coupled dynamics, the overall noise force acting on the monomer stems from the whole rest of the chain and is non-Markovian. Second, since the force does not propagate immediately through the chain, a bond at the grafted end of the chain experiences at the beginning the force smaller than the one that is applied at the pulled terminal. The rupture of a single breakable Morse bond at the fixed wall is affected both by the non-Markovian fluctuations and by the force profile propagation. In contrast, a bond situated at the pulled terminal of the chain feels the instantaneous force, and the deviations from the single-bond rupture statistics are solely due to the non-Markovian character of the noise. Figure 1 shows the most probable rupture force $f_{\max}$ as a function of the number of bonds in the chain N for both situations, revealing quite different behavior. Thus, for a breakable bond at a wall $f_{\max}$ (dashed lines) lies well above the reference value for a single

bond (flat solid line), while for the breakable bond at a pulled terminal $f_{\max}$ lies slightly below the value for the single bond (colored solid lines). We conclude that non-Markovian fluctuations accelerate the rupture process while the retarded force propagation delays it. Since the effect of delay is by an order of magnitude stronger—the stronger the higher the loading rate—we neglect the impact of the non-Markovian character of the fluctuations and neglect correlations introduced by noise by assuming that the rupture of different bonds is independent.

The simulations correspond to solving the set of coupled equations

$$\dot{q}_j = -K_j(q_j - q_{j-1}) + K_{j+1}(q_{j+1} - q_j) + \sqrt{2D}\xi_j + rt\delta_{j,N}, \tag{10}$$

with $j=1,\ldots,N$, $q_0=0$, $K_j(q)=-\partial U_j(q)/\partial q$ and U_j being either the Morse potential (for the breakable bond) or the harmonic potential corresponding to the same stiffness of the bond (for all the others) by use of a Heun integration scheme. A rupture is considered as having taken place when a reaction coordinate $q_{j+1}-q_j$ passed the location of the activation barrier of the breakable bond. Statistics stem from an ensemble of at least 10^3 simulation runs.

B. Chain of N breakable Morse bonds

We pass to a chain of N breakable Morse bonds. Let $W_1[f_j(t)]$ be the probability of the bond j to be intact. Let r be very small, $r \ll 1$ nm/μs^2. Then, we can assume the forces acting on each spring along the polymer chain are virtually the same. This is expected to be true at least for a not too large value of N. The probability that all N bonds are intact is then given by

$$W_N(f) = W_1(f)^N. \tag{11}$$

Then, the probability that a bond breaks in an interval $[f, f+df]$ is $P_N(f)=NW_1(f)^{N-1}P_1(f)$ and is given by the same expression as P_1 with v changed for Nv. Together with (9) we derive the following limiting scaling relation for the most probable rupture force:

$$f_{\max} = f_i\left[1 - \left(\frac{\ln\left(\frac{Nv}{r}\right)}{w}\right)^{2/3}\right]. \tag{12}$$

The experimentally obtained curves of the most probable rupture forces are expected to tend to this scaling relation in the limit of vanishing loading rates. We remark that the scaling predicted by Eq. (12) differs from the one given in [14,27] since the latter is based on the linear theory. A comparison of the experimental results of [14] with the predictions of Eq. (12) shows that it describes the data just as adequately as the linear theory considered in the work, and none of the theories can be falsified at the existing (high) level of the experimental uncertainties.

Let us now turn to higher loading rates. The probability that all N bonds in the chain are still intact under a pulling force at the terminal of the chain being $f(t)$ is then given by

$$W_N\{[f_j(t)]\} = \prod_{j=1}^{N} W_1[f_j(t)]. \tag{13}$$

Passing to the continuum limit ($j \to x$) we obtain

$$W_N(t) = \exp\left(\int_0^N \ln\{W_1[f(x,t)]\}dx\right). \tag{14}$$

Since barrier crossing events are very rare, most of the time the motion of the monomers takes place close to the quadratic potential minima of bond energies. Therefore, we derive the force profile by considering a semi-infinite chain of harmonic springs pulled at $x=0$ with a force $f(t)=rt$, i.e., by solving the following continuum equation for the scalar displacement field $q(x,t)$:

$$\dot{q}(x,t) = c\alpha\Delta_x q(x,t) + rt\delta(x). \tag{15}$$

For not too short chains the impact of the clamped end can be neglected.

Then, the force profile $f(x,t)$ connected to $q(x,t)$ via $f(x,t)=-c\alpha dq/dx$ is given by

$$f(\xi,t) = f(t)\left\{\left[1 - \mathrm{erf}\left(\frac{\xi}{2}\right)\right]\left(1 + \frac{\xi^2}{2}\right) - \frac{\xi}{\sqrt{\pi}}e^{-\xi^2/4}\right\}, \tag{16}$$

with $\xi = x/\sqrt{c\alpha t}$. Linearizing this result near $\xi=0$,

$$f(\xi,t) \simeq f\left(1 - \frac{2\xi}{\sqrt{\pi}}\right), \tag{17}$$

with $f \equiv f(t)$. Together with Eqs. (7) and (14) we obtain

$$W_N(f) = W_0^N \exp\left\{-\frac{vl}{3rw^{2/3}\sqrt{f}}\left[\Gamma\left(\frac{2}{3}, a(f)\right) - \Gamma\left(\frac{2}{3}, a(f)[1 + S(N,f)]^{3/2}\right)\right]\right\}. \tag{18}$$

Here $\Gamma(b,z)=\int_z^\infty t^{b-1}e^{-t}dt$ is the incomplete Γ function, $l=f_i\sqrt{c\alpha\pi/r}$, $a(f)=w(1-f/f_i)^{3/2}$, and $S(N,f)=2N\sqrt{r/(c\alpha\pi)}\sqrt{f}/(f_i-f)$.

We remark, that in the limit $f \to 0$, $W_N(f\to 0) \to W_1^N \to 1$. Finally, the probability density distribution reads as

$$P_N(f) = -W_N(f)\left\{\frac{vl}{6rw^{2/3}f^{3/2}}\left[\Gamma\left(\frac{2}{3}, a(f)\right) - \Gamma\left(\frac{2}{3}, a(f)[1 + S(N,f)]^{3/2}\right)\right] - \frac{vl}{2r\sqrt{f}}\left[\frac{e^{-a(f)}}{f_i} - \left(\frac{1}{f_i} - \frac{N/l}{\sqrt{f}}\right)e^{-a(f)[1+S(N,f)]^{3/2}}\right]\right\}. \tag{19}$$

One might doubt the accuracy of these results based on the linearization assumption, Eq. (17), since for large values of ξ the force $f(x,t)$ can become negative in the region where it essentially must vanish, which is an unphysical result. However, this property of Eq. (17) has no impact on the rupture kinetics. A negative force exponentially suppresses the rate

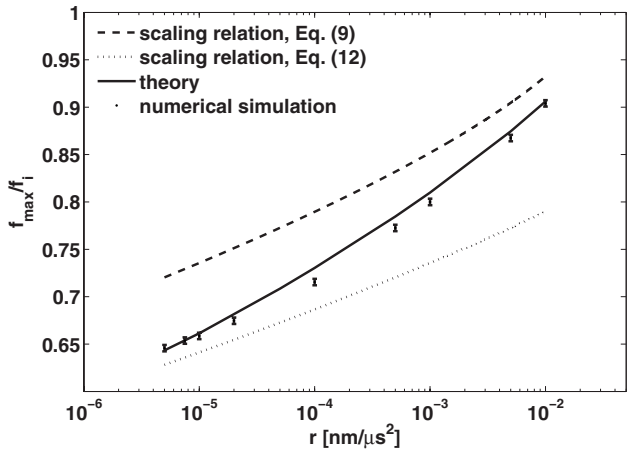

FIG. 2. Most probable rupture force $f_{\max}$ as a function of the loading rate r. The length of the chain is $N=100$. The theoretical values (solid line) are derived from Eq. (19). The remaining parameter values are the same as in Fig. 1.

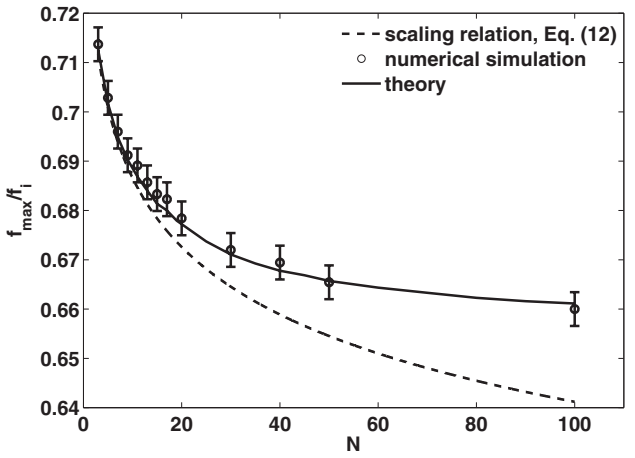

FIG. 3. Most probable rupture force $f_{\max}$ as a function of the chain length N for $r=10^{-5}$ nm/μs^2. The theoretical values (solid line) are derived from Eq. (19). The remaining parameter values are the same as in Fig. 1.

of escape, see Eq. (6), leading to the fact that the corresponding bonds simply do not break. For the rupture kinetics there is therefore no difference between getting negative forces or setting the force to zero, as it is the situation in the physical experiment. To prove this we also performed calculations with a modified profile $f(\xi,t)=(1-2\xi/\sqrt{\pi})\Theta(1-2\xi/\sqrt{\pi})$ instead of Eq. (17), and found practically no difference in the outcome of the theory which for itself agrees very well with the numerical simulations.

In Fig. 2 we present the numerically obtained most probable rupture force $f_{\max}$ as a function of the loading rate r for a chain of length $N=100$. Shown are also the predictions of Eq. (9) (dashed line), of Eq. (12) (dotted line), and the most probable rupture force $f_{\max}$ as derived from Eq. (19) (solid line). In the limit of small r the value of $f_{\max}$ tends to the prediction of Eq. (12): Virtually all bonds account for the rupture process of the chain. In the opposite limit of very large loading rates only a few bonds contribute to rupture (in the extreme limit only the one at the pulled end of the chain) and the scaling of $f_{\max}$ is given by Eq. (9). The crossover behavior is very well reproduced by the theory [Eq. (19)]. Small deviations appear for the intermediate values of r where the exact force profile along the chain plays a role and the linear approximation in Eq. (17) gets slightly inaccurate. Higher-order corrections might resolve this issue.

In Fig. 3 we present the numerically obtained most probable rupture force $f_{\max}$ as a function of the chain length N for $r=10^{-5}$ nm/μs^2. Shown are also the prediction of Eq. (12) (dashed line), and the one of Eq. (19) (solid line). For not too large systems, the predictions of Eq. (12) and of Eq. (19) tend to each other and both describe well the numerical findings. Deviations appear for larger system sizes N, where both the numerical results and the prediction of Eq. (19) saturate. We also show in Fig. 4 that Eq. (19) (solid line) adequately describes the PDF of the actual rupture forces (bars).

The overall behavior shown in Fig. 3 corresponds to a transition from the small-N scaling regime to a saturation after some $N_s(r)$ depending on the loading rate. The value of N_s can be estimated as follows. A single bond rupture is governed by $P_1(f)$ and rupture occurs with highest probability at $f(x,t)=f_{\max}$ with $f_{\max}$ given in Eq. (9). The value of $f_{\max}$ can be translated into the most probable time to break via $t_{\max}=f_{\max}/r$. The distribution $P_1(f)$ is strongly skewed to the left-hand side [10,11], and its variance is given by

$$\sigma_1^2=\frac{2\pi^2 f_i^2}{27w^{4/3}}\frac{1}{\ln\left(\frac{v}{r}\right)^{2/3}}, \tag{20}$$

see Ref. [9]. We then can assume that the rupture of a bond hardly occurs if the corresponding force is $f<f_{\max}-2\sigma_1$. The portion of the chain N_s in which the broken bond is localized is then determined by the condition that the force at the bond number N_s is $f_{\max}-2\sigma_1$ at the time when the first bond is most probably going to break, i.e., $f(N_s,t_{\max})=f_{\max}-2\sigma_1$. Resolving Eq. (17) for the corresponding value of $x=N_s$ we obtain

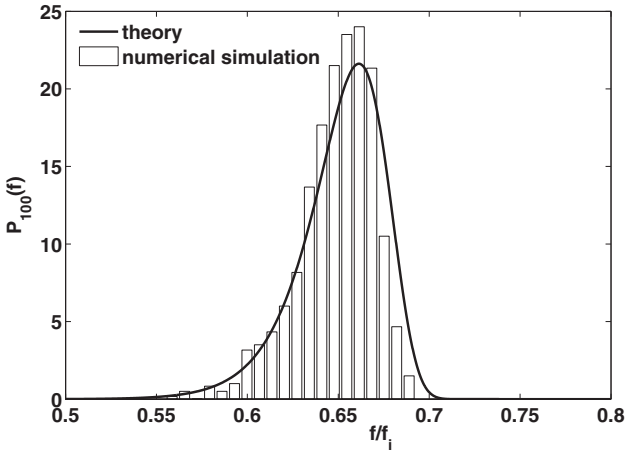

FIG. 4. Probability density distribution of the rupture force for a polymer chain of length $N=100$ and a loading rate $r=10^{-5}$ nm/μs^2. The theoretical values (solid line) are derived from Eq. (19). The remaining parameter values are the same as in Fig. 1.

$$N_s(r) = \left(\frac{c^2\alpha\pi^3}{54r}\right)^{1/2} \frac{1}{\left[\ln\left(\frac{v}{r}\right)w^2\right]^{1/3}} \left[1 - \left(\frac{\ln\left(\frac{v}{r}\right)}{w}\right)^{2/3}\right]^{-1/2}. \tag{21}$$

For $r=10^{-5}$ nm/μs^2 we have $N_s \simeq 100$, in qualitative agreement with the outcome of our numerical simulations, and for $r=10^{-4}$ nm/μs^2 we get $N_s \simeq 35$ (again in agreement with simulations, not shown).

V. SUMMARY

Let us summarize our findings. Compared to single bond breaking, the existence of the chain introduces aspects into rupture dynamics, the most important being the delayed stress propagation along the chain. We show that the most probable rupture force decreases with the length of the chain as $f_{\max} \propto -[\ln(\text{const}\, N/r)]^{2/3}$ and then saturates at a value depending on the loading rate. The results of theoretical considerations are confirmed by numerical simulations. They underline the need to take into account the chain structure of the system under study when interpreting experimental data.

ACKNOWLEDGMENTS

The authors thankfully acknowledge valuable discussions with J. Klafter and M. Urbakh. This research has been supported by DFG within the SFB 555 research collaboration program.

[1] M. Rief, F. Oesterhelt, B. Heymann, and H. E. Gaub, Science **275**, 1295 (1997).
[2] A. D. Mehta, M. Rief, J. A. Spudich, D. A. Smith, and R. M. Simmons, Science **283**, 1689 (1999).
[3] M. Grandbois, M. Beyer, M. Rief, H. Clausen-Schaumann, and H. E. Gaub, Science **283**, 1727 (1999).
[4] S. Cui, C. Albrecht, F. Kühner, and H. Gaub, J. Am. Chem. Soc. **128**, 6636 (2006).
[5] C. Friedsam, A. Wehle, F. Kühner, and H. Gaub, J. Phys.: Condens. Matter **15**, S1709 (2003).
[6] G. Neuert, C. Albrecht, and H. Gaub, Biophys. J. **93**, 1215 (2007).
[7] T. Strunz, K. Oroszlan, R. Schafer, and H.-J. Güntherodt, Proc. Natl. Acad. Sci. U.S.A. **96**, 11277 (1999).
[8] E. Evans, Annu. Rev. Biophys. Biomol. Struct. **30**, 105 (2001).
[9] A. Garg, Phys. Rev. B **51**, 15592 (1995).
[10] O. Dudko, A. Filippov, J. Klafter, and M. Urbakh, Proc. Natl. Acad. Sci. U.S.A. **100**, 11378 (2003).
[11] O. K. Dudko, G. Hummer, and A. Szabo, Phys. Rev. Lett. **96**, 108101 (2006).
[12] C. L. Dias, M. Dubé, F. A. Oliveira, and M. Grant, Phys. Rev. E **72**, 011918 (2005).
[13] F. Kühner and H. Gaub, Polymer **47**, 2555 (2006).
[14] A. Embrechts, H. Schönherr, and G. J. Vancso, J. Phys. Chem. B **112**, 7359 (2008).
[15] E. Evans and K. Ritchie, Biophys. J. **72**, 1541 (1997).
[16] H.-J. Lin, H.-Y. Chen, Y.-J. Sheng, and H.-K. Tsao, Phys. Rev. Lett. **98**, 088304 (2007).
[17] R. W. Friddle, Phys. Rev. Lett. **100**, 138302 (2008).
[18] N. Severin, W. Zhuang, C. Ecker, A. Kalachev, I. Sokolov, and J. Rabe, Nano Lett. **6**, 2561 (2006).
[19] M. Doi and S. Edwards, *The Theory of Polymer Dynamics* (Oxford University Press, Oxford, 1986).
[20] M. Raible, M. Evstigneev, P. Reimann, F. Bartels, and R. Ros, J. Biotechnol. **112**, 13 (2004).
[21] H.-Y. Chen and Y.-P. Chu, Phys. Rev. E **71**, 010901(R) (2005).
[22] Z. Tshiprut, J. Klafter, and M. Urbakh, J. Chem. Phys. **125**, 204705 (2006).
[23] H. Kramers, Physica (Amsterdam) **7**, 284 (1940).
[24] P. Hänggi, P. Talkner, and M. Borkovec, Rev. Mod. Phys. **62**, 251 (1990).
[25] O. Dudko, A. Filippov, J. Klafter, and M. Urbakh, Chem. Phys. Lett. **352**, 499 (2002).
[26] R. Merkel, Phys. Rep. **346**, 343 (2001).
[27] E. Evans and P. Williams, in *Physics of Bio-Molecules and Cells*, edited by H. Flyvbjerg, F. Jülicher, P. Ormos, and F. David (Springer, Berlin, 2002), pp. 145–204.